On-Board Power Management in a Marine Autonomous Surface Vehicle (ASV): Multi-Port Transformer Design

Guillaume Pellecuer, Thierry Martiré, Mickael Petit, Benjamin Loyer

On-Board Power Management in a Marine Autonomous Surface Vehicle (ASV): Multi-Port Transformer Design

Guillaume Pellecuer[1], Thierry Martiré[1], Mickael Petit[2], Benjamin Loyer[2]

[1] IES, Montpellier University, CNRS UMR 5214, France

[2] SATIE, ENS Paris Saclay, CNAM, CNRS UMR8029, France

Corresponding author: Guillaume Pellecuer, guillaume.pellecuer@umontpellier.fr

Abstract

This paper deals with the design of the magnetic component of an isolated bidirectional multiportconverter. This converter is intended to be embedded in an autonomous surface marine vehicle with a power rating in the kilowatt range and is intended to exchange power between photovoltaic panels, a lithium battery and the propulsion system in which the motors can also be operated as a tidal turbine. This magnetic component is a three-port symmetrical three-phase transformer that allows to interface three three-phase inverters with a six-step control. The converter is galvanically isolated and can operate in a fully bi-directional way. Phase shifting of the inverters allows the power flow between them to be adjusted.

1 Introduction

The development of UAVs and ASVs is complicated by the amount and availability of onboard power, which is an essential element for the operation of the vehicle. The space available on these exploration vehicles is relatively limited and high power density converter architectures must be used to reliably and efficiently power the ASV.

A three-port power management system may enable the advantages of the photovoltaic source and storage to be intelligently combined to perfectly manage the redistribution of instantaneous power in the system or to use storage as a way of buffering the power flow from the primary source [1,4].

The use of storage elements also makes it possible to size the primary source solely on the basis of the average power of the load and not only on the basis of the peak power draw of the load, as the storage can supply the difference very quickly and thus avoid oversizing the primary energy source[2, 3, 1]. Finally, the storage can be used as a back-up energy source when the primary source is not available.

A three-phase, magnetically isolated three port converter in which the number of inductive elements that usually contribute significantly to the weight and volume of the converter is minima therefore appears to be well suited to power management in a small, autonomous on-board system. The magnetic component at the heart of the system is a three-port symmetrical three-phase transformer to interface three three-phase inverters with full-wave control, so the converter is galvanically isolated and can operate fully bi-directionally as shown in Fig. 1.

The phase shift of the converter commands allows the power flow to be directed between the converters and therefore to the DC sources if they allow it. The three three-phase systems are therefore slightly shifted according to the transfer requirements.

A power converter such as this one has already been described in [5] but the magnetic component was a high frequency symmetrical transformer

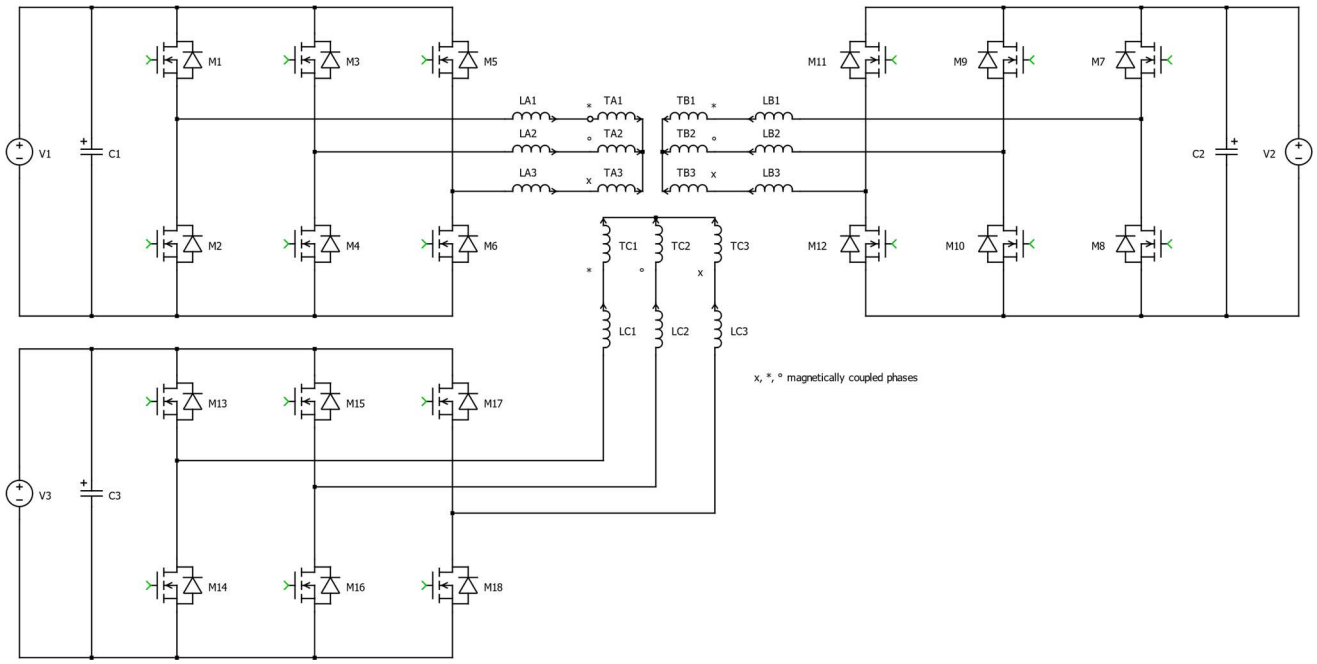

Fig. 1*:* Complete schematic of the converter

with coaxial windings which requires a large number of toroidal cores and a complicated winding to make up for the availability of cores with the right shape for the transformer.

In the following sections a more conventional transformer structure and a planar winding is presented. Fig. 2 shows an exploded view of the magnetic core of the transformer wich was made by sawing commercially available ETD cores with a diamond saw to recover the central cylindric leg. Then the resulting ferrite cylinders were glued onto type I cores.

2 Three port transformer model

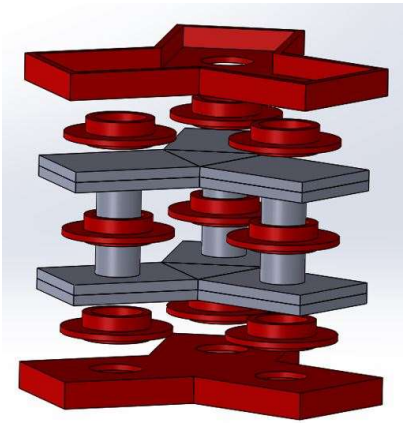

Fig. 2: Exploded view of the magnetic component (grey) and its plastic supports (red)

As mentioned before, the converter consists of three inverters connected by a specially designed transformer whose primary and secondary can be connected in star or delta and as there is no inter-phase coupling the component study can be conducted on a per phase basis.

As shown in Fig. 3, on one leg of the transformer there are three electrically independent phases but magnetically coupled to each other and to the other legs through various mutual inductances. In the following, the currents fed by the inverters are assumed to form a balanced three-phase sine system, we will have, for example, for inverter a: $i_{1a} + i_{2a} + i_{3a} = 0$.

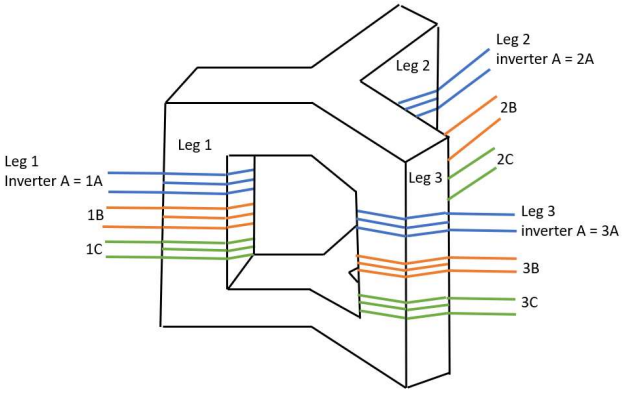

Fig. 3: Inverters phases and windings arrangement on the transformer

For example, to write the magnetic flux through winding 1a (inverter a, phase 1), the self-inductance must be taken into account, as well as the

mutuals linking this coil to the 8 others in the transformer (the mutual between winding 1a and 2b, for example, will be noted M_{1a2b}). Fig. 4 shows how

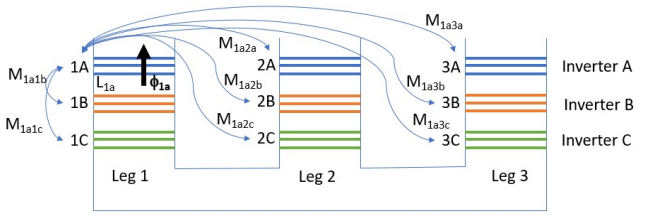

Fig. 4: Self and mutual inductances related to phase a of inverter 1 and its winding

the mutuals related to phase 1 of inverter A and its winding are placed and as shown in Eq. 1.

$$\begin{aligned}\phi_{1a} = L_{1a}.i_{1a} &+ M_{1a2a}.i_{2a} \\ &+ M_{1a3a}.i_{3a} \\ &+ M_{1a1b}.i_{1b} \\ &+ M_{1a2b}.i_{2b} \\ &+ M_{1a3b}.i_{3b} \\ &+ M_{1a1c}.i_{1c} \\ &+ M_{1a2c}.i_{2c} \\ &+ M_{1a3c}.i_{3c}\end{aligned} \quad (1)$$

By doing the same for the other 8 windings, we can obtain the (9x9) matrix of inductances of this transformer.

$$\begin{pmatrix} L_{1a} & M_{1a2a} & M_{1a3a} & M_{1a1b} & M_{1a2b} & M_{1a3b} & M_{1a1c} & M_{1a2c} & M_{1a3c} \\ M_{2a1a} & L_{2a} & M_{2a3a} & M_{2a1b} & M_{2a2b} & M_{2a3b} & M_{2a1c} & M_{2a2c} & M_{2a3c} \\ M_{3a1a} & M_{3a2a} & L_{3a} & M_{3a1b} & M_{3a2b} & M_{3a3b} & M_{3a1c} & M_{3a2c} & M_{3a3c} \\ M_{1b1a} & M_{1b2a} & M_{1b3a} & L_{1b} & M_{1b2b} & M_{1b3b} & M_{1b1c} & M_{1b2c} & M_{1b3c} \\ M_{2b1a} & M_{2b2a} & M_{2b3a} & M_{2b1b} & L_{2b} & M_{2b3b} & M_{2b1c} & M_{2b2c} & M_{2b3c} \\ M_{3b1a} & M_{3b2a} & M_{3b3a} & M_{3b1b} & M_{3b2b} & L_{3b} & M_{3b1c} & M_{3b2c} & M_{3b3c} \\ M_{1c1a} & M_{1c2a} & M_{1c3a} & M_{1c1b} & M_{1c2b} & M_{1c3b} & L_{1c} & M_{1c2c} & M_{1c3c} \\ M_{2c1a} & M_{2c2a} & M_{2c3a} & M_{2c1b} & M_{2c2b} & M_{2c3b} & M_{2c1c} & L_{2c} & M_{2c3c} \\ M_{3c1a} & M_{3c2a} & M_{3c3a} & M_{3c1b} & M_{3c2b} & M_{3c3b} & M_{3c1c} & M_{3c2c} & L_{3c} \end{pmatrix} \quad (2)$$

This matrix only contains values that are easily accessible through the use of an impedance analyser.

The inter-leg mutual inductances of the same inverter (A here) are assumed to be the same and we note $M_{1a2a} = M_{1a3a} = M_a$, we then obtain:

$$\begin{aligned} L_{1a}.i_{1a} + M_{1a2a}.i_{2a} + M_{1a3a}.i_{3a} \\ = L_{1a}.i_{1a} + M_a.i_{2a} + M_a.i_{3a} \\ = (L_{1a} - M_a).i_{1a} \end{aligned} \quad (3)$$

We define Lc_a the cyclic inductance which takes into account the effect of the other two phases of the inverter a with $Lc_a = L_{1a} - M_a$.

This result is possible provided that the currents are sinusoidal. However, the three-phase system prohibits the 3rd harmonic. The leakage inductances filter the currents as a 1st order, the impedance at harmonic 5 (1st non-zero harmonic) is 5 times larger than that of the fundamental. The amplitude of the voltage 5th harmonic is 5 times smaller than that of the fundamental. We can conclude that the amplitude of the current 5th harmonic is 25 times smaller than that of the fundamental and that the currents are sinusoidal.

Inter-leg and inter-inverter mutuals are also assumed to be identical ($M_{1a2b} = M_{1a3b} = M_{ab}$) with M_{ab} : Mutual inductance between legs and between two inverters. M_{1a1b} is the mutual on the same leg and between two inverters, then:

$$\begin{aligned} M_{1a1b}.i_{1b} + M_{1a2b}.i_{2b} + M_{1a3b}.i_{3b} \\ = (M_{1a1b} - M_{ab}).i_{1b} \end{aligned} \quad (4)$$

Defining Mc_{ab} the mutual cyclic inductance between converters A and B that reflects the impact of the windings fed by converter B on those of converter a we have $Mc_{ab} = M_{1a1b} - M_{ab}$

On the third part of ϕ_{1a}, assuming again that the inter-leg and inter-inverter mutuals are identical ($M_{1a2c} = M_{1a3c} = M_{ac}$) we will have:

$$\begin{aligned} M_{1a1c}.i_{1c} + M_{1a2c}.i_{2c} + M_{1a3c}.i_{3c} \\ = (M_{1a1c} - M_{ac}).i_{1c} \end{aligned} \quad (5)$$

The cyclic inductance between inverter C and inverter A is noted Mc_{ac} with $Mc_{ac} = M_{1a1c} - M_{ac}$. And like the previous one, it reflects the impact of the windings fed by the C converter on those of the A converter.

Finally, the magnetic flux of Eq. 1 can then be written:

$$\phi_{1a} = Lc_a.i_{1a} + Mc_{ab}.i_{1b} + Mc_{ac}.i_{1c} \quad (6)$$

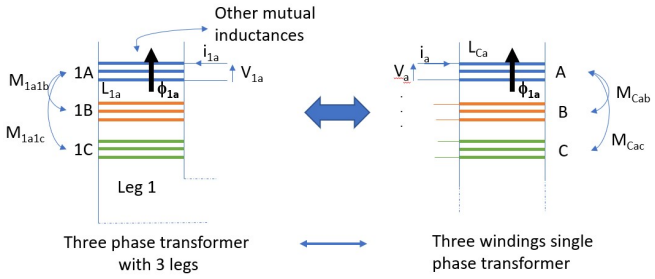

Fig. 5: Three phase to single phase transformer conversion

This expression is now equivalent to what we have for a single-phase transformer with 3 windings.

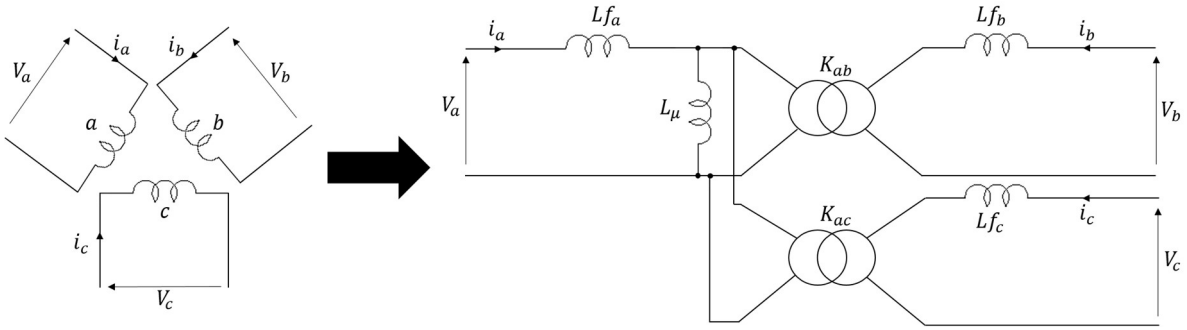

Fig. 6: Full model of the three windings transformer

The inductance matrix can now be written as Eq. 7 shows and allows the conversion of a three-phase transformer to an equivalent single-phase transformer with three windings on the same core as shown in Fig. 5. By circular permutation, we find all the elements of the new inductance matrix (Eq.7):

$$\begin{pmatrix} V_a \\ V_b \\ V_c \end{pmatrix} = \begin{pmatrix} Lc_a & Mc_{ab} & Mc_{ac} \\ Mc_{ab} & Lc_b & Mc_{bc} \\ Mc_{ac} & Mc_{bc} & Lc_c \end{pmatrix} . \frac{d}{dt} \begin{pmatrix} i_a \\ i_b \\ i_c \end{pmatrix} \quad (7)$$

With the matrix in equation 7 and the definition of its elements, it will now be possible to relate the magnetizing inductance and leakage inductances of the single-phase 3-winding system [6] (Fig. 6) to the matrix of inductances and thus to measurable quantities.

Using the diagram in Fig. 6 it is possible to relate the voltages across the windings to the magnetizing inductance and leakage inductances of the component and:

$$\begin{aligned} V_a &= \left(L_\mu + Lf_a\right).\frac{di_a}{dt} + K_{ab}.L_\mu.\frac{di_b}{dt} \\ &\quad + K_{ac}.L_\mu.\frac{di_c}{dt} \\ V_b &= K_{ab}.L_\mu.\frac{di_a}{dt} + \left(K_{ab}^2.L_\mu + Lf_b\right).\frac{di_b}{dt} \\ &\quad + K_{ab}.K_{ac}.L_\mu.\frac{di_c}{dt} \\ V_c &= K_{ac}.L_\mu.\frac{di_a}{dt} + K_{ab}.K_{ac}.L_\mu.\frac{di_b}{dt} \\ &\quad + \left(K_{ac}^2.L_\mu + Lf_c\right).\frac{di_c}{dt} \end{aligned} \quad (8)$$

With $K_{ab} = \frac{V_b}{V_a} = \frac{i_a}{i_b}$ and $K_{ac} = \frac{V_c}{V_a} = \frac{i_a}{i_c}$

These equations can be represented as a matrix system which only contains quantities that can now be calculated using the inductance matrix of Eq. 2.

$$\begin{pmatrix} V_a \\ V_b \\ V_c \end{pmatrix} = \begin{pmatrix} L_\mu + Lf_a & K_{ab}.L_\mu & K_{ac}.L_\mu \\ K_{ab}.L_\mu & K_{ab}^2.L_\mu + Lf_b & K_{ab}.K_{ac}.L_\mu \\ K_{ac}.L_\mu & K_{ab}.K_{ac}.L_\mu & K_{ac}^2.L_\mu + Lf_c \end{pmatrix} . \frac{d}{dt} \begin{pmatrix} i_a \\ i_b \\ i_c \end{pmatrix} \quad (9)$$

Using Eq. 7 and Eq. 9 we obtain a system of 6 equations with 6 unknowns:

$$\begin{aligned} &(1)\ Lc_a = L_\mu + Lf_a \\ &(2)\ Lc_b = K_{ab}^2.L_\mu + Lf_b \\ &(3)\ Lc_c = K_{ac}^2.L_\mu + Lf_c \\ &(4)\ Mc_{ab} = K_{ab}.L_\mu \\ &(5)\ Mc_{ac} = K_{ac}.L_\mu \\ &(6)\ Mc_{bc} = K_{ab}.K_{ac}.L_\mu \end{aligned} \quad (10)$$

And finally, the transformation ratios, magnetizing inductances and leakage inductances can be calculated:

$$\begin{aligned} K_{ab} &= \frac{Mc_{bc}}{K_{ac}.L_\mu} = \frac{Mc_{bc}}{Mc_{ac}} \\ K_{ac} &= \frac{Mc_{bc}}{K_{ab}.L_\mu} = \frac{Mc_{bc}}{Mc_{ab}} \\ L_\mu &= \frac{Mc_{bc}}{K_{ab}.K_{ac}} = \frac{Mc_{ac}.Mc_{ab}}{Mc_{bc}} \\ Lf_a &= Lc_a - L_\mu = Lc_a - \frac{Mc_{ac}.Mc_{ab}}{Mc_{bc}} \\ Lf_b &= Lc_b - K_{ab}^2.L_\mu = Lc_b - \frac{Mc_{ab}.Mc_{bc}}{Mc_{ac}} \\ Lf_c &= Lc_c - K_{ac}^2.L_\mu = Lc_c - \frac{Mc_{ac}.Mc_{bc}}{Mc_{ab}} \end{aligned} \quad (11)$$

In [7,8], it has been shown that an N branch transformer can be described with a so-called T model using N+1 branches of inductances.

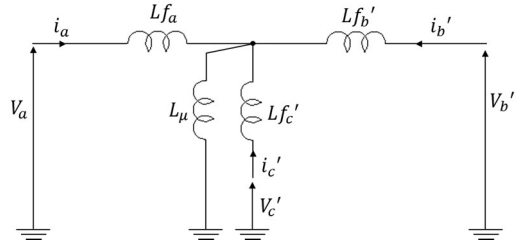

Fig. 7: T-model of the three windings transformer

In the case of the equivalent three-winding transformer presented in the previous calculations, the T-model can be used and the equivalent circuit has one leg for the magnetizing inductance, one for the primary leakage inductance and two for the secondary leakage inductance as shown in Fig. 7. Theoretically, the magnetizing inductance is much greater than the leakage inductances

The equivalent source voltages at the B and C secondaries and the related leakage inductances are given by Eq. 12.

$$\begin{aligned} Lf_b' &= \frac{Lf_b}{K_{ab}^2} & Lf_c' &= \frac{Lf_c}{K_{ac}^2} \\ i_b' &= K_{ab}.i_b & i_c' &= K_{ac}.i_c \\ V_b' &= \frac{V_b}{K_{ab}} & V_c' &= \frac{V_c}{K_{ac}} \end{aligned} \quad (12)$$

3 Calculation of the power delivered by the sources

To carry out this calculation, we will use the diagram in fig. 7, the T-model. The power calculation is done for one leg of the inverters A, B, C. A multiplication by 3 will give the total power.

Hereafter, V_M is the midpoint voltage, V_a is the phase origin and the voltages V_b and V_c are respectively phase shifted by an angle φ_{ab} and φ_{ac} with respect to V_a. Using Kirchhoff's laws we have:

$$\begin{aligned} V_a - Lf_a.i_a - V_M &= 0 \\ V_b - Lf_b.i_b - V_M &= 0 \end{aligned} \quad (13)$$

$$V_c - Lf_c.i_c - V_M = 0$$

$$i_a + i_b + i_c = i_{L_\mu} = \frac{V_M}{jL_\mu\omega}$$

And then :

$$V_M = \frac{1}{3 + \frac{L_f}{L_\mu}}(V_a + V_b + V_c) \quad (14)$$

And by injecting the complex voltage notation ($V_a = [V_m; 0°], V_b = [V_m; \varphi_{ab}], V_c = [V_m; \varphi_{ac}]$) into Eq. 14 it leads to:

$$V_M = \frac{V_m}{3 + \frac{L_f}{L_\mu}}(1 + \cos(\varphi_{ab}) + \cos(\varphi_{ac}) + j\sin(\varphi_{ab}) + j\sin(\varphi_{ac})) \quad (15)$$

And

$$i_a = \frac{-V_m}{L_f\omega\left(3 + \frac{L_f}{L_\mu}\right)}\left[\sin(\varphi_{ab}) + \sin(\varphi_{ac}) + j\left(2 + \frac{L_f}{L_\mu} - \cos(\varphi_{ab}) - \cos(\varphi_{ac})\right)\right] \quad (16)$$

In generator convention (no conjugate current), we can write that:

$$P = \frac{1}{2}Real(\underline{V} \times \underline{I}) \quad (17)$$

hence,

$$P_a = \frac{-V_m^2}{2L_f\omega\left(3 + \frac{L_f}{L_\mu}\right)}[\sin(\varphi_{ab}) + \sin(\varphi_{ac})] \quad (18)$$

The same thing can be applied to inverters B and C ($\varphi_{ba} = -\varphi_{ab},\ \varphi_{ca} = -\varphi_{ac},\ \varphi_{bc} = -\varphi_{cb} = \varphi_{ac} - \varphi_{ab}$).
Hence, the total power expression for each inverter is:

$$P_a = \frac{-3V_m^2}{2L_f\omega\left(3 + \frac{L_f}{L_\mu}\right)}[\sin(\varphi_{ab}) + \sin(\varphi_{ac})] \quad (19)$$

$$P_b = \frac{-3V_m^2}{2L_f\omega\left(3+\frac{L_f}{L_\mu}\right)}[\sin(-\varphi_{ab}) + \sin(\varphi_{ac}-\varphi_{ab})]$$

$$P_c = \frac{-3V_m^2}{2L_f\omega\left(3+\frac{L_f}{L_\mu}\right)}[\sin(-\varphi_{ac}) + \sin(\varphi_{ab}-\varphi_{ac})]$$

With the conventions used for these calculations, the power is negative if the source draws power and positive when it delivers power.

4 Transformer design

4.1 Finite elements simulation

In order to validate our assumptions about the design of the transformer, we have built a prototype and have characterised it, but first we have chosen to model it using the finite element method [9] with the COMSOL Multiphysics software.
The simulated geometry was created using the 3D building interface of comsol. The magnetic core is made with three 3 cylindric leg obtained from ETD59 cores in 3C90 material and PLT64/50/5. The windings were simulated by multiturn coils with 2 turn like in the prototype. The software's built-in SPICE simulator was used to simulate the inverters and the coils were supplied with sinusoidal voltages with an amplitude of 20V and a frequency of 50kHz.

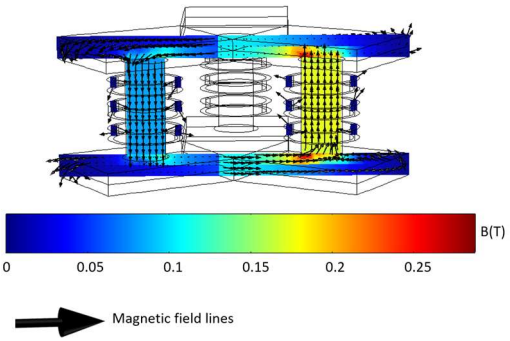

Fig. 8: Simulation of a power exchange (A and B each send 150W to C), induction in the transformer

The 3C90 magnetic material constituting the transformer has been described by a Jiles Artheton hysteresis model integrated in the software [10] allowing to take into account the magnetic hysteresis characteristic of the ferrite material and thus to calculate the iron losses (eddy currents, magnetic losses).

The first results showed that the planned design would achieve the intended power and indeed allow power to be transferred between the inverters. As shown in the example illustrated in Fig. 8, inverters A and B should send about 300W equally to inverter C. The induction in the transformer shows that the operating point is far from saturation and that even more power can be transferred without significant losses. For this operating point, we have about 15W of losses or an efficiency of 95%.

4.2 Realization of the transformer

As previously mentioned, the transformer was made by sawing commercially available cores to match the dimensions used in the simulation.

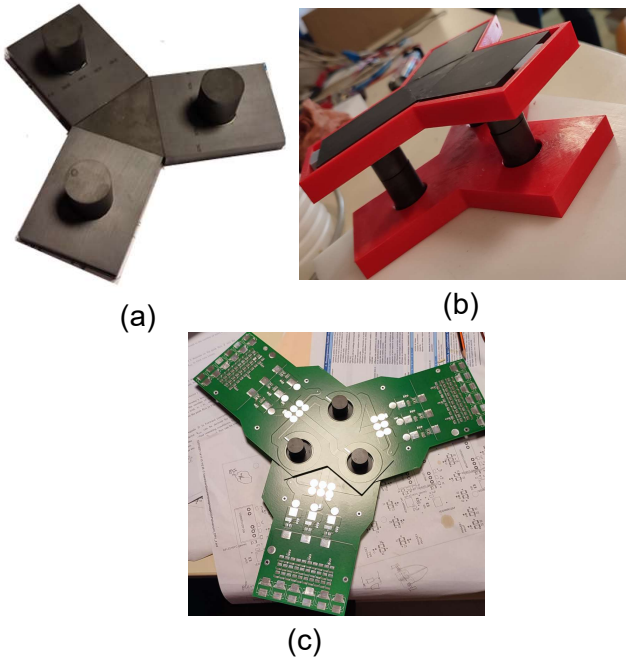

Fig. 9: The three port transformer prototype

A struers secotom diamond saw was used to obtain the columns, which are in fact composed of two cylinders from ETD59 cores placed end to end. The flat parts of the transformer are made up of PLT64 flat rectangles and the junction between the flats was obtained by sawing a PLT64 to make an equilateral triangle whose side length is equal to the smallest length of the PLT64. All these elements were then glued together to form a half shell (Fig. 9a). Two half-transformers were manufactured and assembled using 3D printed parts (Fig. 9b). The windings are drawn directly onto the PCB of the inverter. This PCB is drilled with holes and

plugged directly onto the transformer columns (Fig. 9c).

4.3 Inductance matrix measurement

To measure the inductance matrix, the windings were connected in star and an HP4194a impedance analyser was used. The measurement and connection diagram of the impedance analyser is given in Fig. 10. Although in principle the matrix is symmetrical, the 81 self and mutual inductances were measured (3 inverters with 3 phases per inverter and 3 transformer legs with 3 windings per leg) in order to highlight possible imbalances.

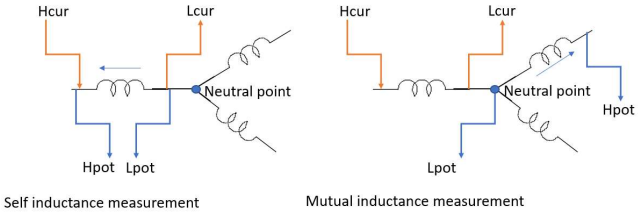

Fig. 10: Measurement schematics

Hcur/Lcur are the current injection ports of the HP4194a and Lpot/Hpot are the measurement ports. The inductance matrix was measured for a frequency of 50kHz which is the intended switching frequency of the inverters. The resulting inductance matrix is given in Fig. 11. (All values in μH).

	1a	2a	3a	1b	2b	3b	1c	2c	3c
1A	3,37	-0,914	-0,967	3	-1,08	-1,1	2,86	-1,1	-1,12
2A	-0,939	3,35	-1,22	-1,05	3,22	-1,35	-1,08	3,08	-1,37
3A	-0,998	-1,23	3,76	-1,098	-1,36	3,41	-1,1	-1,39	3,28
1B	3,02	-1,06	-1,1	3,19	-1,1	-1,12	3,03	-1,08	-1,13
2B	-1,08	3,22	-1,36	-1,1	3,35	-1,4	-1,09	3,24	-1,38
3B	-1,11	-1,36	3,4	-1,1	-1,35	3,52	-1,12	-1,35	3,42
1C	2,91	-1,08	-1,13	3	-1,12	-1,15	3,22	-1,11	-1,14
2C	-1,1	3,12	-1,39	-1,12	3,2	-1,39	-1,07	3,4	-1,38
3C	-1,13	-1,39	3,3	-1,15	-1,41	3,39	-1,1	-1,35	3,68

Fig. 11: Inductance matrix of the transformer

From these measurements it appears that, as expected, the matrix is symmetrical, taking into account the geometry. Moreover, the inductance matrix must be block symmetrical and this is what we obtain with measurement errors that are not large (<1%).

The self-inductances of the same three-phase system are close and the mutual inductances on the same leg are close. Furthermore, they are close to the self-inductances, which indicates that there is little inter-phase leakage and that the component is close to a true transformer, and not to coupled inductances in the flyback sense. Finally, the mutual inductances of the same three-phase system are close to one third of the self-inductance, which means that there is little inter-leg leakage.

4.4 Experimental equivalent T-model

Using this matrix of inductances experimentally measured with the HP4194a impedance analyser and using the relationships determined in the previous equations it is possible to calculate the elements of the matrix of equation 7 as shown in Eq. 20. (All values in μH)

$$\begin{pmatrix} V_a \\ V_b \\ V_c \end{pmatrix} = \begin{pmatrix} 4{,}48 & 4{,}09 & 3{,}97 \\ 4{,}09 & 4{,}46 & 4{,}13 \\ 3{,}97 & 4{,}13 & 4{,}56 \end{pmatrix} . \frac{d}{dt} \begin{pmatrix} i_a \\ i_b \\ i_c \end{pmatrix} \qquad (20)$$

All the windings have 2 turns and are made on PCB. We therefore have $K_{ab} = K_{ac} = 1$ and we can determine all the elements of the equivalent T-model.

L_μ = 3,93μH, L_{fa} = 0,552μH, $L_{fb'}$ = 0,19μH, $L_{fc'}$ = 0,534μH.

Sawing ferrites, which are very hard ceramic materials, is difficult and without grinding the sawn surfaces it is impossible to obtain a perfect surface finish. Finally, the manufacturing tolerances of commercial ferrites are of the order of a millimeter and it is therefore difficult to perfectly align them thus explaining the dissymmetries that are finally obtained between the different inductances. Nevertheless, we have introduced the values obtained from the measurements into the PSIM simulation schematic in Fig. 12.

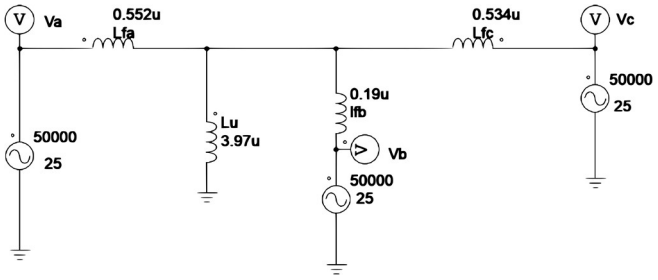

Fig. 12: Psim circuit used for the simulation of the T-model

All the sources have a frequency of 50kHz and a peak voltage value of 25V. V_b has a phase shift of 8° with respect to V_a and V_c an offset of 13° (chosen arbitrarily).

With the chosen conventions in the previous calculations, power is considered negative when the source is absorbing power and positive when it is delivering power. The simulation in Fig. 13 shows that inverter A absorbs 225.9W and that inverters B and C supply 51.5W and 175W respectively. There is therefore a transfer of power between the

different inverters, which can be adjusted by modifying the phase shift between their respective controls. However, it can also be seen that the asymmetry in the leakage inductances strongly unbalances the transfer.

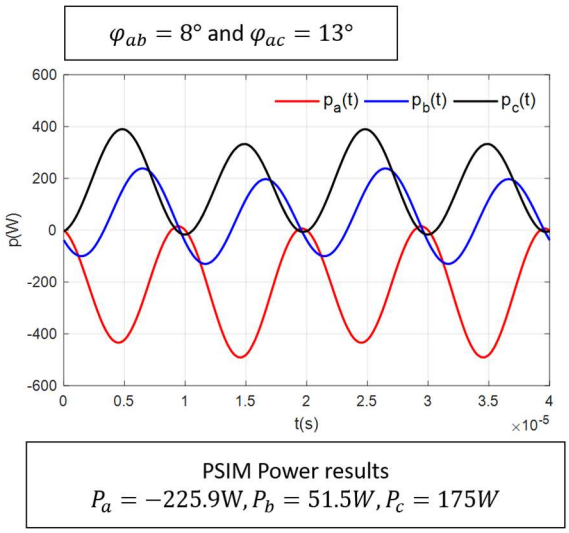

Fig. 13: Simulation for identical phase shifts between Va and Vb and Vc.

If, as in the simulation in Fig. 14, the phase shifts of Vb with respect to Va and Vc with respect to Va are identical, it can be seen that one of the two sources delivers much more power than the other (232.8W for B and 82.2W for C for total power of 314W in A), which can eventually lead to involuntary saturation of a part of the transformer. It is therefore very important that the construction be absolutely symmetrical so that the different inductances of the circuit are also symmetrical.

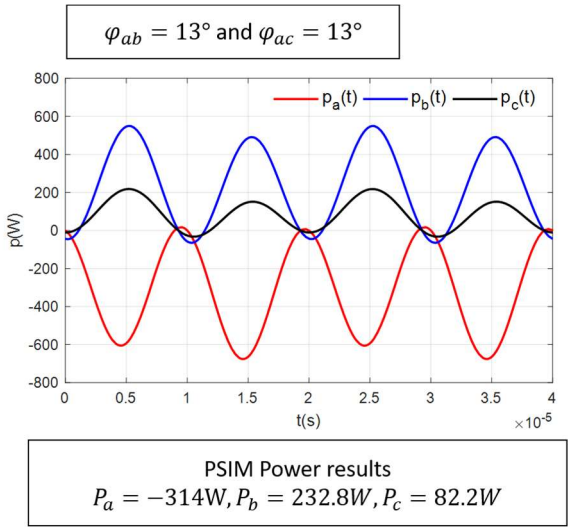

Fig. 14: Simulation for phase shifts of 8 degrees between Va and Vb and 13 degrees between Va and Vc.

5 Conclusion

In this paper we have proposed a three-port system based on the use of three-phase inverters and a multi-port transformer to facilitate the exchange of energy between the converters. The system was modelled analytically. The component was produced by sawing and gluing commercial elements, then characterised with an impedance analyser to determine its inductance matrix and a so-called T-model whose elements were calculated from this matrix was proposed and simulated. In the light of the results obtained, it is clear that this type of component can be used in multi-port converters but that it must be made with particular care, so that it is as symmetrical as possible in order that the inductances themselves are symmetrical and the power transfer is easily adjustable without the need to significantly vary the phase shifts between the inverters.

6 Acknowledgment

The ASV research was supported supported by Occitanie region in a FEDER program N : ESR R&S DF-000035-2017- 006565.

7 References

[1] D. Liu et H. Li, “A Three-Port Three-Phase DC-DC Converter for Hybrid Low Voltage Fuel Cell and Ultracapacitor”, in Proc. IEEE Ind. Electron., p. 2558 – 2563, déc. 2006.

[2] H. Tao, J. Duarte et M. Hendrix, “High- Power Three-Port Three-Phase Bidirectional DC-DC Converter”, in Conference Record - IAS Annual Meeting (IEEE Industry Applications Society), p. 2022 – 2029, oct. 2007.

[3] J. Duarte, M. Hendrix et M. Simoes, “Three-Port Bidirectional Converter for Hybrid Fuel Cell Systems”, Power Electronics, IEEE Transactions on, vol. 22, p. 480 – 487, avril 2007.

[4] M. Michon, J. L. Duarte, M. Hendrix and M. G. Simoes, "A three-port bi-directional converter for hybrid fuel cell systems," 2004 IEEE 35th Annual Power Electronics Specialists Conference (IEEE Cat. No.04CH37551), 2004, pp. 4736-4742, Vol.6, doi: 10.1109/PESC.2004.1354836.

[5] G. Waltrich, J. L. Duarte et M. A. M. Hendrix, “Design of symmetrical highfrequency coaxial wound transformer for multiport converters”, in Proceedings 5th IEEE Young Researchers Symposium, YRS2010, 29-30-03, Leuven,

(United States), p. 1–7, Institute of Electrical and Electronics Engineers, 2010.

[6] A. Ganz, "A Simple, Exact Equivalent Circuit for the Three-Winding Transformer," in IRE Transactions on Component Parts, vol. 9, no. 4, pp. 212-213, December 1962, doi: 10.1109/TCP.1962.1136764.

[7] C. Sun, N. H. Kutkut, D. W. Novotny, et D. M. Divan, « General equivalent circuit of a multi-winding co-axial winding transformer », in IAS '95. Conference Record of the 1995 IEEE Industry Applications Conference Thirtieth IAS Annual Meeting, 1995, vol. 3, p. 2507-2514 vol.3. doi: 10.1109/IAS.1995.530622.

[8] H. Tao, A. Kotsopoulos, J. L. Duarte and M. A. M. Hendrix, "A Soft-Switched Three-Port Bidirectional Converter for Fuel Cell and Supercapacitor Applications," 2005 IEEE 36th Power Electronics Specialists Conference, 2005, pp. 2487-2493,doi: 10.1109/PESC.2005.1581982

[9] Buchau, A., & Rucker, W. M. (2011, October). Analysis of a Three-Phase Transformer using COMSOL Multiphysics and a Virtual Reality Environment. In Proceedings of the 2011 COMSOL Conference, Stuttgart, Germany (Vol. 13, pp. 1-6).

[10] S. Saeed, R. Georgious, and J. Garcia, "Modeling of Magnetic Elements Including Losses-Application to Variable Inductor," Energies, vol. 13, no. 8, 2020. DOI: 10.3390/en13081865.